Behavioral/Cognitive

# Noninvasive Suppression of Responses to Threat Using Focused Ultrasonic Waves

Keisuke Tsunoda,[1,2,3] Taylor D. Webb,[4] Carter Lybbert,[1] Matthew G. Wilson,[1] Brian J. Mickey,[1,5] and Jan Kubanek[1,2]

[1]Department of Biomedical Engineering, University of Utah, Salt Lake City, Utah 84112, [2]Department of Psychiatry, Washington University School of Medicine, St. Louis, Missouri 63110, [3]Graduate School of Arts and Sciences, The University of Tokyo, Meguro-ku, Tokyo 153-8902, Japan, [4]Department of Radiology and Imaging Sciences, University of Utah, Salt Lake City, Utah 84112, and [5]Department of Psychiatry, Huntsman Mental Health Institute, University of Utah, Salt Lake City, Utah 84112

**The processing of threat- and fear-related responses is known to involve the amygdala and the bed nucleus of the stria terminalis. Malignant activity in these nuclei is associated with several important disorders, including generalized anxiety disorder and post-traumatic stress disorder. A noninvasive approach to modulate these deep brain circuits could provide novel treatment options for these disorders, but current noninvasive approaches cannot access these targets directly. This study modulates these nuclei using transcranial low-intensity focused ultrasound in nonhuman primates. The ultrasound was delivered into these circuits prior to an emotional stimulus (neutral, submissive, or threatening monkey faces or snake images) while measuring the system's autonomic response using pupil size. We found that the neuromodulation substantially reduced the pupillary responses to threat images. The effect was specific to threat face images and specific to focused ultrasound; it was not observed for other types of images or for unfocused or no-ultrasound. Thus, focused ultrasound targeting fear circuits can suppress responses to threat images. This approach could be developed into noninvasive treatments of disorders that affect these circuits.**

*Key words:* **amygdala; bed nucleus of the stria terminalis; noninvasive; transcranial; ultrasound neuromodulation**

**Significance Statement**

**Responses to threat often become maladaptive, leading to disorders that include generalized anxiety disorder and post-traumatic stress disorder. The neural circuitry underlying fear processing is situated deep in the brain, and has thus been difficult to access using existing neuromodulation approaches. This study shows that low-intensity focused ultrasound targeting these deep brain circuits in non-human primates specifically suppresses responses to threat images. This approach could provide a noninvasive way to modulate processing of fear.**

## Introduction

The amygdala and the bed nucleus of the stria terminalis (BNST) are interconnected limbic nuclei that integrate and transmit emotional and stress-related signals (Lebow and Chen, 2016; Kamali et al., 2023). These deep brain nuclei play a critical role in generalized anxiety disorder, post-traumatic stress disorder (PTSD), specific phobias, and depression (Baron-Cohen et al., 2000; Straube et al., 2007; Banihashemi et al., 2015; Ferri et al., 2017; Fonzo and Etkin, 2017; Garcia, 2017; Kolla et al., 2017; Fox and Shackman, 2019; Henigsberg et al., 2019).

The amygdala is known to be involved in detection of threat and regulation of emotions (Hur et al., 2019). Neuroimaging and single-unit recording studies indicate that the amygdala selectively responds to emotionally salient and attention-drawing stimuli, including faces and aversive images (Hariri et al., 2002; Rutishauser et al., 2011; Alexandra Kredlow et al., 2022). In particular, monkeys with lesions in the amygdala exhibit deficits in detecting facial features that are important for threat evaluation, and show suppressed pupillary dilation (Dal Monte et al., 2015). Furthermore, images of snakes have been shown to increase neuronal activity in the monkey amygdala (Dinh et al., 2022), and lesions in the amygdala or anterior cingulate sulcus selectively impair emotional responses to artificial snakes (Izquierdo et al., 2005; Rudebeck et al., 2006). These findings together suggest that the amygdala plays a key role in modulating neural responses to fear-related stimuli.

Received April 18, 2025; revised Aug. 12, 2025; accepted Aug. 25, 2025.

Author Contributions:K.T., C.L., M.G.W., B.J.M., and J.K. designed research; K.T. and T.D.W. performed research; K.T. and T.D.W. analyzed data; K.T. wrote the first draft of the paper; K.T., T.D.W., C.L., M.G.W., B.J.M., and J.K. edited the paper; K.T. wrote the paper.

This work was funded by grants from the NIH (R00NS100986, RF1NS128569, and F32MH123019), the Focused Ultrasound Foundation (10059775), and by the Margolis Foundation. We thank Caroline Garrett for veterinary assistance and Tyler Davis for surgical assistance. We thank Prof. Olga Dal Monte and Prof. Naho Konoike for sharing the monkey face image dataset used in this experiment. K.T. was supported by a JSPS Cross-border Postdoctoral Fellowship (22KJ1769).

J.K. is a cofounder of SPIRE Therapeutics. The remaining authors declare no competing financial interests.

Correspondence should be addressed to Keisuke Tsunoda at keisuke.tsunoda@utah.edu.

This paper contains supplemental material available at: https://doi.org/10.1523/JNEUROSCI.0776-25.2025

https://doi.org/10.1523/JNEUROSCI.0776-25.2025

The BNST has also been associated with disorders of fear processing, including anxiety disorders, PTSD, and phobias (Straube et al., 2007; Buff et al., 2017; Rabellino et al., 2018). Anatomically, the BNST is considered an extension of the central nucleus of the amygdala and is known to be involved in stress, anxiety, and emotional processing. It has been implicated in responses to uncertain threats and sustained fear, contributing to the maintenance of prolonged states of stress and anxiety (Avery et al., 2016; Lebow and Chen, 2016).

The amygdala and, by extension, the BNST are considered key targets for control of the associated disorders. Indeed, deep brain stimulation of the amygdala shows appreciable improvements in PTSD symptoms (Langevin et al., 2016; Koek et al., 2024). Nonetheless, to eventually provide these treatments to patients at a large scale, the neuromodulation would ideally be noninvasive. However, current noninvasive approaches, including transcranial magnetic stimulation or transcranial direct or alternating current stimulation, do not have the necessary field strength and resolution at depth. Recently, transcranial focused ultrasound has emerged as a technique capable of targeting deep brain regions with millimeter- and millisecond-scale precision, which could provide precise, circuit-directed treatments of the involved deep brain circuits (Sarica et al., 2022; Riis et al., 2023; Matt et al., 2024; Riis et al., 2024a).

Studies in humans and non-human primates have demonstrated that ultrasound can modulate brain function associated with visual circuits, mood networks, and motivation pathways, as well as brain regions implicated in neurological and mental diseases (Hameroff et al., 2013; Legon et al., 2014, 2018; Kubanek et al., 2020). In particular, ultrasound stimulation targeting deep brain nuclei has been reported to suppress somatosensory evoked potentials and alter post-stimulation resting-state connectivity (Dallapiazza et al., 2018; Folloni et al., 2019).

Given the above, we hypothesize that ultrasound modulation of the amygdala and BNST will influence affective responses to fear-related stimuli. In a previous amygdala lesion study (Dal Monte et al., 2015), the effects of the lesions were particularly pronounced for threat images. We therefore predict maximal effects of ultrasound on threatening images.

## Methods

*Animals.* The study involved two male macaque monkeys (*Macaca mulatta*), aged 8 and 9 years, and weighing 15.0 and 10.8 kg, respectively. All procedures adhered to protocols approved by the Institutional Animal Care and Use Committee at the University of Utah.

*Targets.* This stimulation used the Remus system (Webb et al., 2022), an ultrasonic phased array designed to deliver ultrasound precisely and reproducibly into specific deep brain regions. Remus is a 256-element, 480–800 kHz phased array that is mounted to the head of awake behaving monkeys (Fig. 2*A*). The system features four critical properties for the purpose of this study and nonhuman primate applications. First, the fixed positioning of the array with respect to the head ensures repeated and reproducible modulation of the intended deep brain targets from session to session. The reproducible targeting is crucial for the proposed work that delivers stimulation to deep brain regions across many sessions. Second, the behaving primate is critical for the assessment of the ultrasonic effects on responses to fear. Third, the large brain of the primate facilitates selective targeting of specific deep brain regions (Fig. 2*C*). And fourth, findings obtained in primates at 480 kHz are directly translatable into clinical trials using adjacent frequency (e.g., 650 kHz) human brain systems (Ghanouni et al., 2015; Riis et al., 2023, 2024a,b). The system has been described in prior work (Webb et al., 2022), and a summary is provided in Table 1 and below.

In this approach, a custom head frame is affixed to the subject's skull using four surgically implanted titanium pins. The location of the metallic pins was chosen such as not to interfere with the ultrasound beam (Fig. 2*A*, Fig. S1). To achieve head fixation, the frame is attached to a primate chair (Crist Instruments, Hagerstown, MA) using two steel bars. The frame houses a 256-element ultrasound transducer array (Doppler Electronic Technologies, Guangzhou, China; Webb et al., 2022), with acoustic coupling provided by a cryogel (Lee et al., 2014). This configuration allows the array to be reliably positioned in the same location during each session, enabling consistent collection of behavioral and neural data under head fixation. Ultrasound is directed to specific deep brain regions electronically using targeting software, without the need to move the transducer or the subject (Webb et al., 2022).

The targeted brain regions included the bilateral amygdala and bilateral BNST (four sites in total). The ultrasound focus was targeted at the basal nucleus of the amygdala. The half-power beamwidth of the acoustic focus measured in a water tank is $1 \times 3.75 \times 3.75$ mm in the left/right, anterior/posterior, and superior/inferior dimensions, respectively (Webb et al., 2022). The monkey amygdala is approximately $8 \times 5 \times 8$ mm in size (Saleem and Logothetis, 2012), and the stimulation coordinate center was determined to allow stimulation across the amygdala

**Table 1. Stimulation parameters**

| | | | |
|---|---|---|---|
| **Transducer description** | | | |
| Transducer manufacturer | Doppler Electronic Technologies | | |
| Transducer model | HP-500K-256-BE | | |
| Transducer center frequency | 650 (operated at 480) kHz | | |
| Transducer geometry | Semicircular, 65 mm radius of curvature | | |
| Number of elements | 256 | | |
| Element distribution | The elements are 4 × 4 mm square and the distance between elements is 4.2 mm. The array is arranged in a 32 × 8 configuration. | | |
| **Drive system description and settings** | | | |
| Operating frequency | 480 kHz | | |
| Output voltage | 18.12 V | | |
| Drive system | Verasonics Vantage 256 | | |
| Coupling method | 6% PVA gel is compressed between the subject's head and the transducer. | | |
| Focal position settings | | Monkey B | Monkey E |
| | Left amygdala: | [−9 −16 62] | [−9 −9 68.5] |
| | Right amygdala: | [6.5 −15 62] | [ 9 −9 68.5] |
| | Left BNST: | [−4.5 −13.5 51.5] | [−2.5 −7 56.5] |
| | Right BNST: | [1 −13.5 51.5] | [ 1 −7 56.5] |
| | Coordinates are in mm and represent the [Left/Right, Anterior/Posterior, Superior/Inferior] position relative to the center of the transducer surface. | | |
| **Pulse timing parameters for each target** | | | |
| Pulse duration | 30 ms | | |
| Duty cycle | 5% | | |
| Total duration | 30 s | | |

**Estimated *in situ* pressure amplitude**

| Estimation method | Scaled from MR thermometry data | | |
|---|---|---|---|
| | Amygdala | BNST | Unfocused |
| Spatial-peak pressure (MPa) | 0.34 | 0.68 | 0.01 |
| $I_{SPTA}$ (W/cm$^2$) | 0.18 | 0.74 | $1.6 \times 10^{-4}$ |
| $I_{SPPA}$ (W/cm$^2$) | 3.69 | 14.84 | $3.2 \times 10^{-3}$ |
| Mechanical index | 0.49 | 0.99 | 0.014 |
| Temperature rise (°C) | 0.01 | 0.02 | $3.0 \times 10^{-4}$ |

subnuclei. The approximate dimensions of the BNST are 2 × 2 × 2 mm in the same respective dimensions. Target coordinates were individually adjusted for each animal based on prior MR thermometry information (see below) and remained consistent across sessions.

The targeting of the amygdala and BNST was based on MR thermometry, reported previously (Webb et al., 2022). Briefly, MR thermometry sonications were calibrated to induce a temperature increase of 2–3°C. The thermometry sonications, conducted at the transducer's center frequency of 650 kHz. This minimal temperature increase and the substantial time gap minimize the likelihood of thermometry influencing subsequent neuromodulation outcomes. Due to time constraints during these experiments, we were only able to confirm targeting of three locations (the two lateral geniculate nuclei and one additional target). Thus, MR thermometry confirms targeting of the left BNST in subject B and the right amygdala in subject E, while targeting of the other two regions was performed by measuring their location relative to the lateral geniculate nucleus.

The neuromodulation sessions followed the thermometry sessions by at least 6 months.

*Behavioral task.* We presented the individual images relatively infrequently to prevent adaptation. Specifically, we interleaved with the image presentation a visual discrimination task (Kubanek et al., 2020) that the monkeys were trained on previously (Webb et al., 2022).

The animals were seated in a custom-designed head-fixed monkey chair in a dark room. Visual stimuli were presented on an LCD monitor positioned 67 cm in front of the monkeys' eyes. Eye position and pupil area were monitored using an EyeLink camera system (Eyelink, SR Research). The data were sampled at 100 Hz. To standardize acquisition timing relative to image onset, the data were downsampled to 40 Hz.

In the visual discrimination task, the monkeys first acquired a central fixation target. After a short delay, the first target (a 0.5° × 0.5° gray square) appeared either on the left or right side of the screen, 6° from the fixation center. After a random delay (0–0.1 s), a second target with identical parameters appeared on the opposite side. The order of target appearance (left-first or right-first) was randomized across trials. Both targets remained on the screen until the monkey made a choice. To receive a liquid reward, the monkeys were required to make a saccade to one of the targets within 1 s of the first target's appearance. The saccade had to fall within a 2° acceptance window and remain within this window for at least 0.1 s. The next trial commenced 1.0 s after the reward was delivered. The reward delivery valve was open for 15 ± 8 ms, depending on the animal. Monkeys received 311 ± 92 ml of liquid reward per session. If this did not meet the individual minimum daily requirement, additional water was provided following a session. To minimize the pupillary constriction response due to luminance changes, a background image was presented in which the subsequently displayed image (with a visual angle of 5.1° × 5.3°) was pixel-wise shuffled. A 3° × 3° black hole was placed at the center, ensuring that the fixation point remained visible (see the fixation screen at the top of Fig. 1).

In the image presentation trials, the monkeys first fixated on a central target before an image was displayed (Fig. 1). The images subtended a visual angle of 5.1° × 5.3°. After maintaining fixation for 0.26 to 2.76 s, the pixel-wise shuffled background image disappeared, and the monkeys were presented with an image for 1.5 s. The presented face images included three ecologically relevant facial expressions—neutral, submissive, and threatening faces—as well as images of snakes. The monkey face image datasets were obtained from Dal Monte et al. (2015), Konoike et al. (2020), and Taubert and Japee (2024), while the snake images were sourced and cropped from the Geneva Affective Picture Database (Dan-Glauser and Scherer, 2011). To eliminate extraneous background features that could be distracting, all face stimuli were embedded in a black oval mask. During the 1.5 s presentation period, the monkeys were free to explore or ignore the presented images. After the presentation period, a 20 s inter-trial interval (ITI) was introduced. The ITI was chosen to be 20 s to provide sufficient time to evaluate potential long-term effects of the ultrasound stimulation on the pupil diameter. During this interval, the screen remained black. Subsequently, a shuffled image was presented for the next image presentation trial. No rewards were given during the image presentation tests.

The delivery of ultrasound was initiated while the monkey was engaged in the visual discrimination task. The ultrasound was delivered for 30 s, followed by image presentation. The time of image onset was randomized to minimize anticipation. Image presentation trials were initiated by the monkey's spontaneous fixation. Consequently, there was a median interval of 1.4 s (interquartile range: 1.00–2.54 s) between the end of the ultrasound and the onset of image presentation. Sessions took between 30 to 40 min. The interval between successive image presentations was at least 2 min. During this interval, the monkeys voluntarily performed the visual discrimination task, and no conditioned stimuli were presented to prevent ultrasound or image anticipation.

An image presentation trial was considered valid if the monkey successfully maintained fixation on the initial fixation point. If fixation was broken during the required fixation period, the trial was discarded. The image was presented repeatedly until the monkey successfully achieved fixation. All valid trials were included in the analysis. Each monkey underwent 8–11 sessions per ultrasound stimulation condition.

The total number of image presentation trials varied across sessions (min: 5, max: 14, and mean: 9.6). To prevent anticipation, the number of presented images was varied across sessions. We analyzed a total of 41–51 trials per ultrasound conditions for each of the four images (Fig. S2). Trials were excluded if a hardware or software error was detected or if the operator manually delivered a reward during fixation or image presentation. Such rewards were occasionally given at the operator's discretion to maintain the subject's attention.

*Protocol.* Three conditions—focused ultrasound stimulation targeting the BNST and amygdala of both sides, no-ultrasound condition (control), and an unfocused-ultrasound condition as an active sham—were randomized between sessions (Fig. 2*B*). Within each session, the same ultrasound stimulation condition was repeated across all image presentation trials. Ultrasound stimuli had a 480 kHz carrier frequency and an in situ amplitude of 0.34 MPa in amygdala and 0.68 MPa in BNST.

Stimulation was applied sequentially to the four targets (the left and right amygdala and the left and right BNST) in a repeating cycle (1 → 2 → 3 → 4 → 1 → . . .), with each stimulation period lasting 30 ms followed by a 120 ms interval before the next target (Fig. 2*D*). This resulted in a cycle duration of 150 ms per target and a full four-target cycle of 600 ms. Each target was thus sonicated for 30 ms every 600 ms, repeated over 30 s.

The intensity of the ultrasound at target was estimated based on thermometry results obtained from stimulation of the amygdala and BNST, following the methods outlined in Webb et al. (2022). This approach has been described previously (Webb et al., 2022, 2023), and is therefore summarized here only briefly. In two subjects, the measured temperatures in the targets were combined with Pennes' bioheat equation (Pennes, 1948) to estimate the delivered intensity. The average estimate of intensity across the two subjects was used to estimate an attenuation factor which we then apply in subsequent experiments to estimate the in situ pressure. In these experiments, we targeted 0.34 MPa at focus for the amygdala and 0.68 MPa for the BNST. For amygdala stimulation, the resulting acoustic parameters during each 30 ms pulse were as follows: spatial peak temporal average intensity ($I_{SPTA}$) = 0.18 W/cm$^2$, spatial peak pulse average intensity ($I_{SPPA}$) = 3.69 W/cm$^2$, duty cycle (DC) = 5%, pulse repetition frequency (PRF) = 6.67 Hz, and pulse duration (PD) = 30 ms. For BNST stimulation, the corresponding values were $I_{SPTA}$ = 0.74 W/cm$^2$, $I_{SPPA}$ = 14.84 W/cm$^2$, DC = 5%, PRF = 6.67 Hz, and PD = 30 ms (Table 1).

We evaluated the effects of unfocused-ultrasound as an active sham. The sonications used the same parameters as the verum condition, but the ultrasound was not focused into the targets. Instead, the individual delays for each of the 256 elements were set randomly. The same four-step ultrasound stimulation sequence as in the focused condition was used in the unfocused condition (with four different sets of random phases), resulting in equivalent total pressure delivered into the brain. The sham sonications applied random phases to each element in order to spread the beam throughout the brain. Thus, even though the total power delivered in each case is the same, the sham condition blurs the beam so that each individual brain region experiences very low pressure.

To ensure our random phases did not produce undesirable hot spots near the target, we performed a simple simulation of the array. Our simulation assumes that each transducer element is a point source in a homogeneous medium. The steady-state pressure is then simply a sum of complex exponentials. Using this approach we estimated the intensity at each target during sham stimulus compared to verum stimulus. We find that, at the target, the sham stimulus delivers an average of 0.4% of the intensity delivered during verum stimulus (Fig. S3).

In total, 30 sessions were collected from monkey E and 33 sessions from monkey B. Three sessions of Monkey B with missing data were excluded from the analysis.

*Statistical analysis.* To assess the effects of ultrasound on the pupillary constriction response, we analyzed pupil size changes across four image types: threat, snake, neutral, and submissive. The analysis focused on the time window from 0.5 to 4 s after image onset, in which pupil constriction modulation was observed. The assumption of normality was often violated, based on the Shapiro–Wilk test ($W = 0.994$, $p = 0.025$). We therefore used the non-parametric Kruskal–Wallis test. The analysis was performed by pooling all trials across subjects and sessions. All statistical tests were two-tailed, and significance was set at $p < 0.05$. Statistical analyses were conducted using MATLAB2023b and R version 4.5.1.

## Results

To examine whether ultrasound stimulation of the amygdala and the BNST alters pupillary responses to emotional images in macaques, we delivered transcranial focused ultrasound to these regions prior to the presentation of face and snake images (Fig. 1). We targeted the bilateral amygdala and bilateral BNST using a phased array system (Fig. 2), and evaluated three conditions: (i) focused (ii) unfocused, and (iii) no-ultrasound. We designed the experiment based on a previous finding that amygdala lesions reduce pupillary responses to emotionally salient images, particularly those conveying threat (Fig. 3).

We found that brief pulses of ultrasound targeting the bilateral amygdala and BNST, delivered prior to an image presentation, modulated pupillary constriction (Dal Monte et al., 2015) in an image type-specific manner. Figure 4 presents the changes in pupil size for each image type. The visual stimulus was presented for 1.5 s. The onset of image stimulation induced a pupillary light reflex within the first 0.5 s of each trial, followed by sustained constriction.

In the time window between 0.5 and 4 s, the average pupillary constriction size in the focused ultrasound condition was reduced compared to the no-ultrasound condition by mean ± s.e.m. values of $42.24 \pm 10.58\%$ for threat faces, $8.57 \pm 12.39\%$ for images of snake, $26.35 \pm 15.13\%$ for neutral faces, and $28.82 \pm 10.32\%$ for submissive faces. In contrast, in the unfocused-ultrasound condition, the average pupillary constriction size was changed compared to the no-ultrasound condition by $-5.19 \pm 9.83\%$ for threat faces, $11.10 \pm 12.40\%$ for images of snake, $9.31 \pm 14.62\%$ for neutral faces, and $24.18 \pm 10.23\%$ for submissive faces.

Prior research showed that stimulation of the amygdala produces a particularly strong suppressive effect on responses to threatening facial expressions (Dal Monte et al., 2015). We therefore hypothesized that the effect of the ultrasound condition would be most pronounced for the threat image type. We applied the Kruskal–Wallis analysis to examine the effect of ultrasound on the reaction to threat images. A significant effect was indeed observed [$\chi^2$ (2) = 9.38, $p = 0.009$]. We also evaluated the effects of ultrasound on the other image conditions. We found no effect in those cases [images of snake: $\chi^2(2) = 0.21$, $p = 0.899$; neutral faces: $\chi^2(2) = 2.07$, $p = 0.356$; submissive faces: $\chi^2(2) = 4.95$, $p = 0.084$]. The strong effect observed for threat images survived the Holm correction for multiple comparisons.

Post hoc analysis using Dunn's test for the threat condition revealed that the pupil size effect for focused ultrasound condition was significantly different from the no-ultrasound ($p = 0.013$) and unfocused-ultrasound ($p = 0.007$) conditions.

This modulation of the pupillary constriction response by ultrasound showed a similar trend in both animals (Fig. S4). For Subject E, the modulation of the pupillary response by focused ultrasound, compared to the no-ultrasound condition, was $45.72 \pm 19.71\%$ for threat faces, $13.36 \pm 18.21\%$ for images of snake, $38.36 \pm 26.54\%$ for neutral faces, and

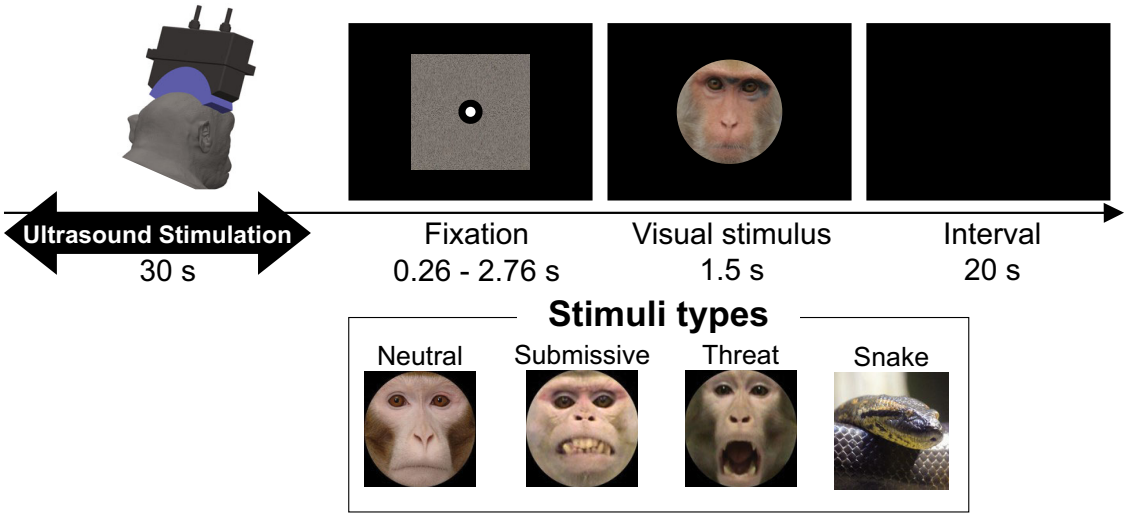


**Figure 1.** Behavioral task. The animal was head-fixed and faced a computer monitor with an ultrasound-conductive gel and an ultrasound transducer positioned on its head. Prior to an image presentation, ultrasound was applied to the the amygdala and BNST for 30 s. Following the ultrasound offset, the monkey initiated the trial by fixating on a central fixation point for 0.26 to 2.76 s (median: 0.48 s, interquartile range: 0.39–0.77 s). Following the fixation period, an image of either a monkey face or a snake was displayed for 1.5 s. The image was centered on the fixation point. During the presentation, the monkey was free to explore the image while a gaze-tracking camera recorded pupil size. The 1.5 s image presentation was followed by a 20 s inter-trial interval. No rewards were given during the image presentation task. The bottom of the figure exemplifies the four different images presented: a neutral, submissive, or threatening face, and a snake.

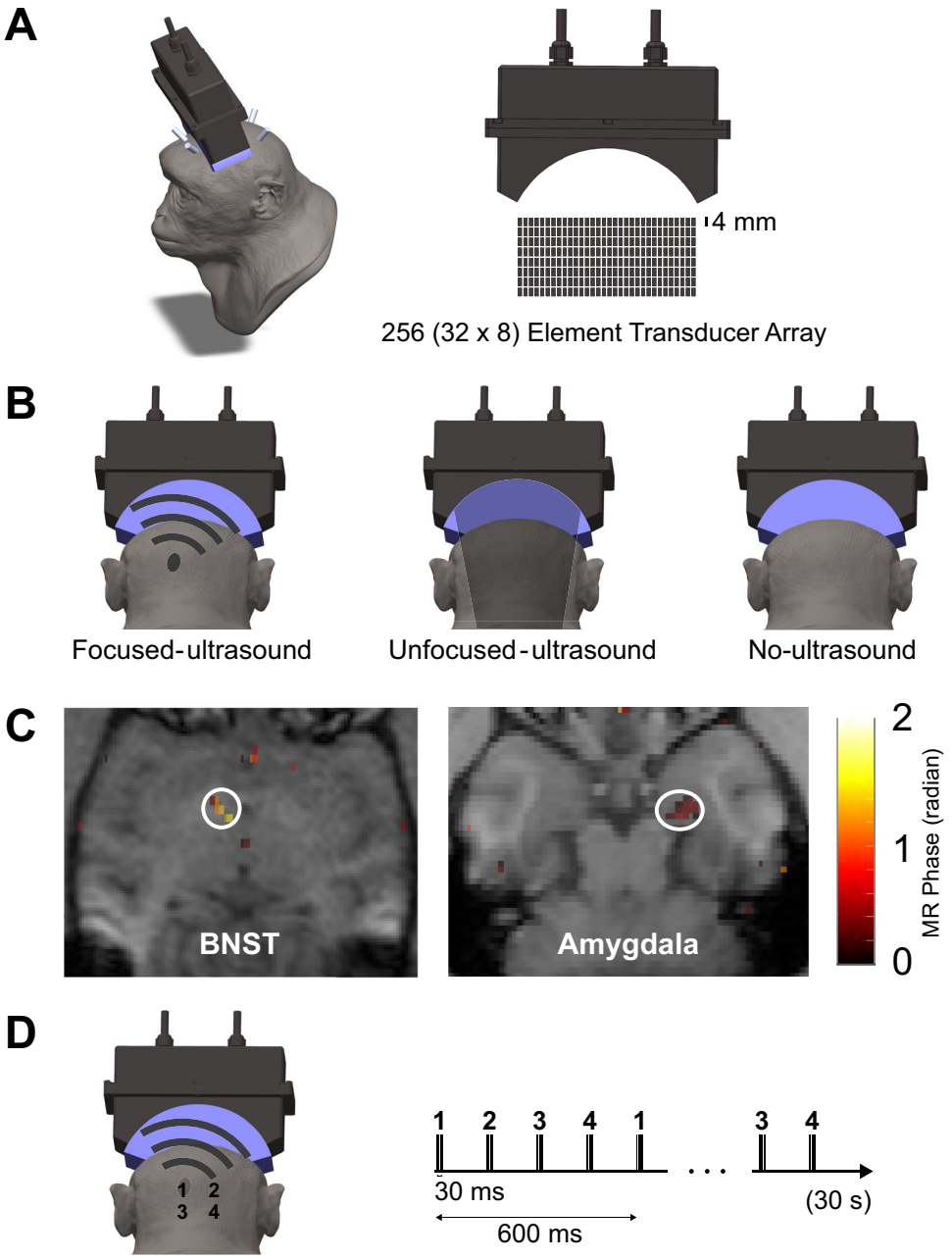


**Figure 2.** Ultrasound stimulation conditions and targeting. ***A***, The monkey's head was fixed using head pins implanted into the skull, and an ultrasound transducer was placed between them. The pins or their base did not interfere with the ultrasound pathway. The transducer consisted of 256 elements. ***B***, An ultrasound transducer was placed on the monkey's head, with an ultrasound-conductive gel applied between the transducer and the head. Three conditions were used: (1) Focused ultrasound: Ultrasound was focused on both the left and right amygdala and the left and right BNST. (2) Unfocused-ultrasound: An active sham control where ultrasound parameters matched the focused condition, but delays for the 256 elements were randomized. (3) No-ultrasound: No-ultrasound stimulation was delivered. ***C***, Selective targeting of the BNST and amygdala, with an MRI thermometry overlay. Images represent data from two monkeys. ***D***, The sequence of the four targets: each stimulus consisted of a 30 ms stimulation period followed by a 120 ms interval. The left and right amygdala and BNST were stimulated in sequence. The targets were stimulated in order over a 30-s period.

23.50 ± 16.95% for submissive faces. For Subject B, the corresponding values were 34.06 ± 10.34% for threat images, 2.23 ± 14.81% for snake images, 21.89 ± 17.02% for neutral images, and 34.10 ± 11.90% for submissive images.

To verify that the threat-specific pupillary modulation effect was not due to the animals averting their gaze away from the images, we compared the total duration of gaze within the image area during stimulus presentation across conditions. No significant differences were found among the conditions for all image types [threat faces: $\chi^2(2) = 0.50$, $p > 0.99$; images of snake: $\chi^2(2) = 2.45$, $p > 0.99$; neutral faces: $\chi^2(2) = 1.04$, $p > 0.99$; submissive faces: $\chi^2(2) = 2.07$, $p > 0.99$, Kruskal–Wallis test].

It has been reported that the extended amygdala is involved in satiety and reinforcer devaluation in goal-directed behavior (Izquierdo et al., 2013; Rhodes and Murray, 2013). To examine whether ultrasonic stimulation influenced motivation, we investigated whether the total amount of reward consumed per session and the number of trials varied across the ultrasound conditions. We found no significant differences in the total trials and amount of reward across the ultrasound conditions [Trial:

$F(2, 57) = 0.232$, $p = 0.794$, One-way ANOVA; reward consumption: $\chi^2(2) = 2.94$, $p = 0.231$, Kruskal–Wallis test].

No adverse effects were observed during or after the stimulation. The animals exhibited normal behavior after the stimulation and participated in the experiments the next day.

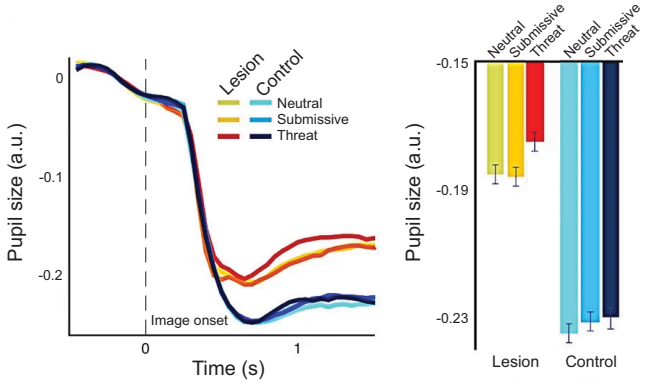


**Figure 3.** Prediction based on a lesion study. Amygdala lesions suppress pupil constriction especially for threatening images. Adapted from Dal Monte et al. (2015), with permission.

## Discussion

This study demonstrated that bilateral stimulation of the amygdala and BNST in monkeys using transcranial low-intensity focused ultrasound selectively suppressed the pupillary response to threatening facial expressions. The effect was specifically observed during focused ultrasound stimulation; there was no effect during unfocused-ultrasound, and no effect for other kinds of stimuli. These findings suggest that ultrasound can modulate deep brain circuits involved in fear processing and consequently modulate specific emotional responses.

### Relationship between pupil dilation and the amygdala-BNST circuit

Changes in pupil size serve as a key indicator of vigilance, arousal, and attentional engagement (Steinhauer et al., 2004). A prior study using amygdala-lesioned monkeys has reported attenuated pupillary constriction in response to viewing various monkey face images (Dal Monte et al., 2015). The effect was strongest for images that represent threat, which is consistent with our findings (Fig. 4). The modulation effect in this study is in the inhibitory direction because it points in the same direction as that observed following amygdala lesions (Dal Monte et al., 2015). We used a relatively

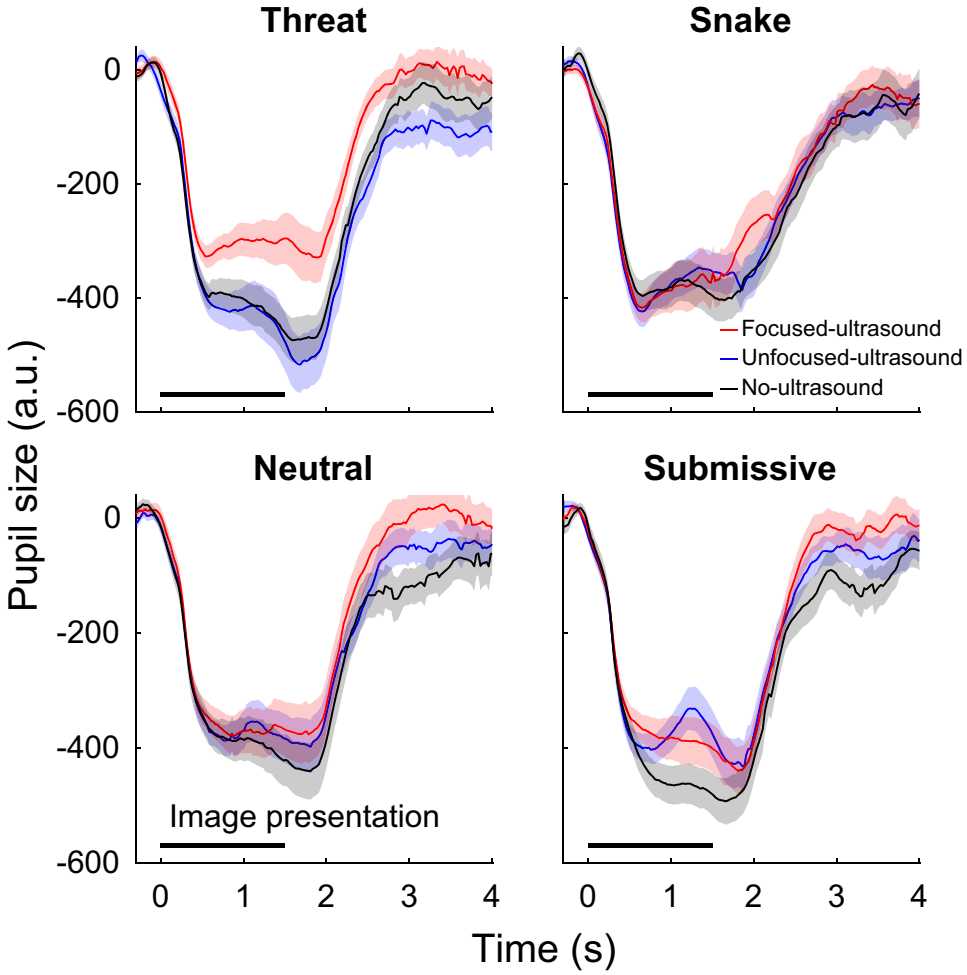


**Figure 4.** Modulation of the amygdala and BNST with focused ultrasound suppresses responses to threat. Time course of the pupil diameter, aligned to image onset. The diameter is quantified with respect to baseline, defined as the 1 s period immediately preceding stimulus presentation. The horizontal black bar indicates the image presentation period. The visual stimulus appeared at time 0 and remained on the screen for 1.5 s. The shaded plots represent the mean ± standard error of pupil size at each time point.

low DC (5%) and stimulus duration (30 ms), which are predicted to elicit neuronal inhibition (Plaksin et al., 2016). Indeed, we found low DC stimuli inhibitory also in our previous non-human primate study (Webb et al., 2023).

The amygdala consists of multiple nuclei with distinct functions. For example, fMRI studies in monkeys have shown that the basolateral amygdala exhibits stronger responses to threatening affiliative facial expressions, and BNST has also been implicated in facial image processing (Hoffman et al., 2007). Ultrasound used in this study may have selectively targeted specific subnuclei, such as the basolateral amygdala. Both the amygdala and BNST are anatomically positioned to regulate core aspects of fear and anxiety, including arousal, behavioral inhibition, and neuroendocrine activity, via dense mono- and polysynaptic projections to the brainstem and subcortical effector regions (Fox et al., 2015; Fudge et al., 2017). The selective suppression of pupillary responses to threatening facial expressions observed in this study may thus reflect modulation of these subnuclei.

Moreover, lateralized functional differences in the amygdala have been reported (Gläscher and Adolphs, 2003; Robinson et al., 2010; Murphy et al., 2020). Future studies should investigate whether the observed suppression of threat-related responses is primarily driven by lateralized differences in specific amygdalar subnuclei or whether the amygdala, BNST, and the broader extended amygdala network collectively contribute to the modulation of emotional responses.

Snake images have been reported to elicit rapid and robust neuronal activity in the amygdala (Dinh et al., 2022). In monkeys, amygdala lesions are known to suppress acute escape responses to snakes (Kalin et al., 2001). Our finding of no modulation by ultrasound is therefore surprising. The absence of ultrasound-induced modulation in pupillary responses to snakes suggests that, unlike socially relevant threatening expressions, the neural substrates underlying autonomic responses in predator-related processing may involve additional brain regions beyond the amygdala and the BNST. Another possibility is that ultrasound stimulation specifically modulated a subregion of the amygdala responsible for fear responses to aggressive conspecifics. In rodents, predator attack threats primarily engage the lateral amygdala and basomedial amygdala, while threats from aggressive conspecifics are processed by a distinct circuit involving the medial amygdala (Gross and Canteras, 2012). However, no studies in primates have explicitly demonstrated that threats from aggressive conspecifics and predators, such as snakes, engage distinct circuits within the amygdala. Given that snakes have been evolutionary predators of primates (Isbell, 2006, 2009) and that conspecific facial threats serve as critical social signals (Burrows, 2008; Dobson, 2009; Dobson and Sherwood, 2011), it is plausible that these threat types are processed in different amygdala subregions. Future research is needed to elucidate the neural mechanisms underlying this distinction.

### Technological advances

Traditional noninvasive brain stimulation techniques, such as TMS, lack the capability to selectively and instantaneously target deep brain regions (Kubanek et al., 2018). By comparison, this study leveraged focused ultrasound to stimulate fear-related circuits situated deep in the brain.

### Implications

This study demonstrated that fear- and anxiety-related nodes could be selectively and rapidly stimulated across both hemispheres, inducing physiological modulation. This finding underscores the potential of ultrasound-based interventions and this ultrasound system (Remus; Webb et al., 2022), for future psychiatric research and cognitive neuroscience, particularly in establishing the contributions of deep networks to emotional processing.

A potential reason for the significant impact on pupillary diameter, a physiological indicator, is that the protocol of continuously stimulating four targets for 30 s may have led to a cumulative effect. To our knowledge, no prior research stimulating the amygdala with ultrasound has reported the modulation of physiological responses to fear stimuli (Folloni et al., 2019; Mahdavi et al., 2023; Chou et al., 2024; Hoang-Dang et al., 2024; Barksdale et al., 2025). It is possible that the cumulative effect from this continuous stimulation of four targets was sufficient to elicit the modulatory effect on the physiological indicator.

Our finding that focused ultrasound suppresses the autonomic response to threat images corroborates recent findings in humans. A study by Rascu et al. (2025), for instance, reported that ultrasound stimulation of the amygdala led to a reduced sensitivity to negative information (Rascu et al., 2025). The pupillary response serves as a direct physiological measure of arousal and engagement with emotionally salient stimuli. Therefore, our observation of a blunted pupillary reaction specifically to threat faces is evidence of a physiological manifestation of this reduced sensitivity. This convergence of findings across species strongly supports that focused ultrasound is a tool to selectively modulate the processing of negative affect within the amygdala and BNST circuits. This provides a potential mechanism for the therapeutic effects observed in humans and suggests the possibility for clinical translation.

### Limitations and future directions

The effects of ultrasound in this study were transient and did not persist across the experimental sessions. While previous research in primates has demonstrated that 40 s of ultrasound can alter functional connectivity between the amygdala and other regions for more than an hour (Folloni et al., 2019), the conditions necessary to induce long-term and sustained changes in the neural activity of the amygdala and BNST at a multi-day level have not yet been identified. To explore the therapeutic potential of ultrasound for psychiatric disorders, such as anxiety disorders and PTSD, future studies should identify stimulation parameters capable of eliciting long-term changes in amygdala and BNST activity. Specifically, expanding the stimulation beyond the 30-s period could produce more sustained effects on the stimulated networks (Riis et al., 2024a).

The targeting of the amygdala and BNST was validated using representative measurements, but spatial discrepancies in the effective stimulation area may occur due to factors such as beam width, tissue absorption, scattering, and phase shifts (Chang et al., 2016; Riis et al., 2022). Additionally, while the estimated parameters provide a reference, the actual power delivered to each target remains uncertain due to potential variations in tissue properties and acoustic transmission. To consistently investigate the modulation effects of ultrasound and the intensity and spatial characteristics of its modulatory effects on nuclei in the future, precise estimation of individual parameters will be required.

We used thermometry data in two subjects (measured in the amygdala of subject E and the BNST of subject B) to estimate the delivered pressure. The actual pressure delivered to each target will vary. Our method partially accounts for this using a simple

simulation to estimate changes in intensity due to the array geometry but the simulation does not account for the effect of the skull. In addition, intensity estimates based on MR thermometry depend on assumed tissue thermal properties and are blurred by the spatial and temporal averaging of the sequence. For these reasons, the stated 0.34 MPa (amygdala) and 0.68 MPa (BNST) pressures should be regarded as informed estimates rather than absolute measurements.

The extended amygdala is known to play a role in satiety and reinforcer devaluation during goal-directed actions (Izquierdo et al., 2013; Rhodes and Murray, 2013). We therefore investigated whether our ultrasound stimulation affected these behaviors by analyzing task performance and reward consumption across conditions. Our analysis showed no significant effect of focused ultrasound on either the number of trials completed or the total amount of reward consumed. This null finding suggests that our focal stimulation was insufficient to alter these complex behaviors. Given reports that such motivated behaviors also rely on broader networks including the orbitofrontal cortex (Baxter et al., 2000), future research aiming to modulate satiety and reinforce devaluation with ultrasound may need to target these larger-scale networks.

One challenge in targeting deep brain nuclei with ultrasound in humans is the precision of stimulation and individual anatomical variability. Despite the high spatial resolution of ultrasound, inter-individual differences in skull thickness and shape may introduce acoustic aberrations that distort focal positioning and intensity (Ammi et al., 2008; Riis et al., 2022). These challenges are particularly critical when targeting small subnuclei within the BNST and amygdala, where millimeter-scale errors could lead to unintended stimulation of adjacent regions. The observed effects of ultrasound on pupillary responses suggest that pupillometry could serve as an objective biomarker to assess whether ultrasound accurately engages its intended target.

### Conclusion

This study demonstrated that transcranial low-intensity focused ultrasound can selectively modulate deep brain circuits involved in fear processing. The findings could lead to developments of noninvasive modulation strategies to ameliorate the symptoms of the associated disorders.

## Data and Materials Availability

Behavioral data have been deposited in Figshare (DOI: 10.6084/m9.figshare.28711166.v1).

## References


Alexandra Kredlow M, Fenster RJ, Laurent ES, Ressler KJ, Phelps EA (2022) Prefrontal cortex, amygdala, and threat processing: implications for PTSD. Neuropsychopharmacology 47:247–259.

Ammi AY, Mast TD, Huang IH, Abruzzo TA, Coussios CC, Shaw GJ, Holland CK (2008) Characterization of ultrasound propagation through ex-vivo human temporal bone. Ultrasound Med Biol 34:1578–1589.

Avery SN, Clauss JA, Blackford JU (2016) The human BNST: functional role in anxiety and addiction. Neuropsychopharmacology 41:126–141.

Banihashemi L, Sheu LK, Midei AJ, Gianaros PJ (2015) Childhood physical abuse predicts stressor-evoked activity within central visceral control regions. Soc Cogn Affect Neurosci 10:474–485.

Barksdale BR, Enten L, DeMarco A, Kline R, Doss MK, Nemeroff CB, Fonzo GA (2025) Low-intensity transcranial focused ultrasound amygdala neuromodulation:a double-blind sham-controlled target engagement study and unblinded single-arm clinical trial. Mol Psychiatry 30:1–15.

Baron-Cohen S, Ring HA, Bullmore ET, Wheelwright S, Ashwin C, Williams SC (2000) The amygdala theory of autism. Neurosci Biobehav Rev 24:355–364.

Baxter MG, Parker A, Lindner CC, Izquierdo AD, Murray EA (2000) Control of response selection by reinforcer value requires interaction of amygdala and orbital prefrontal cortex. J Neurosci 20:4311–4319.

Buff C, Brinkmann L, Bruchmann M, Becker MPI, Tupak S, Herrmann MJ, Straube T (2017) Activity alterations in the bed nucleus of the stria terminalis and amygdala during threat anticipation in generalized anxiety disorder. Soc Cogn Affect Neurosci 12:1766–1774.

Burrows AM (2008) The facial expression musculature in primates and its evolutionary significance. Bioessays 30:212–225.

Chang WS, Jung HH, Zadicario E, Rachmilevitch I, Tlusty T, Vitek S, Chang JW (2016) Factors associated with successful magnetic resonance-guided focused ultrasound treatment: efficiency of acoustic energy delivery through the skull. J Neurosurg 124:411–416.

Chou T, et al. (2024) Transcranial focused ultrasound of the amygdala modulates fear network activation and connectivity. Brain Stimul 17:312–320.

Dallapiazza RF, Timbie KF, Holmberg S, Gatesman J, Lopes MB, Price RJ, Miller GW, Elias WJ (2018) Noninvasive neuromodulation and thalamic mapping with low-intensity focused ultrasound. J Neurosurg 128:875–884.

Dal Monte O, Costa VD, Noble PL, Murray EA, Averbeck BB (2015) Amygdala lesions in rhesus macaques decrease attention to threat. Nat Commun 6:10161.

Dan-Glauser ES, Scherer KR (2011) The Geneva Affective Picture Database (GAPED): a new 730-picture database focusing on valence and normative significance. Behav Res Methods 43:468–477.

Dinh HT, Meng Y, Matsumoto J, Setogawa T, Nishimaru H, Nishijo H (2022) Fast detection of snakes and emotional faces in the macaque amygdala. Front Behav Neurosci 16:839123.

Dobson SD (2009) Socioecological correlates of facial mobility in nonhuman anthropoids. Am J Phys Anthropol 139:413–420.

Dobson SD, Sherwood CC (2011) Correlated evolution of brain regions involved in producing and processing facial expressions in anthropoid primates. Biol Lett 7:86–88.

Ferri J, Eisendrath SJ, Fryer SL, Gillung E, Roach BJ, Mathalon DH (2017) Blunted amygdala activity is associated with depression severity in treatment-resistant depression. Cogn Affect Behav Neurosci 17:1221–1231.

Folloni D, Verhagen L, Mars RB, Fouragnan E, Constans C, Aubry JF, Rushworth MFS, Sallet J (2019) Manipulation of subcortical and deep cortical activity in the primate brain using transcranial focused ultrasound stimulation. Neuron 101:1109–1116.e5.

Fonzo GA, Etkin A (2017) Affective neuroimaging in generalized anxiety disorder: an integrated review. Dialogues Clin Neurosci 19:169–179.

Fox AS, Oler JA, Tromp DPM, Fudge JL, Kalin NH (2015) Extending the amygdala in theories of threat processing. Trends Neurosci 38:319–329.

Fox AS, Shackman AJ (2019) The central extended amygdala in fear and anxiety: closing the gap between mechanistic and neuroimaging research. Neurosci Lett 693:58–67.

Fudge JL, Kelly EA, Pal R, Bedont JL, Park L, Ho B (2017) Beyond the classic VTA: extended amygdala projections to DA-striatal paths in the primate. Neuropsychopharmacology 42:1563–1576.

Garcia R (2017) Neurobiology of fear and specific phobias. Learn Mem 24:462–471.

Ghanouni P, Pauly KB, Elias WJ, Henderson J, Sheehan J, Monteith S, Wintermark M (2015) Transcranial MRI-guided focused ultrasound: a review of the technologic and neurologic applications. AJR Am J Roentgenol 205:150–159.

Gläscher J, Adolphs R (2003) Processing of the arousal of subliminal and supraliminal emotional stimuli by the human amygdala. J Neurosci 23:10274–10282.

Gross CT, Canteras NS (2012) The many paths to fear. Nat Rev Neurosci 13:651–658.

Hameroff S, Trakas M, Duffield C, Annabi E, Gerace MB, Boyle P, Lucas A, Amos Q, Buadu A, Badal JJ (2013) Transcranial ultrasound (TUS) effects on mental states: a pilot study. Brain Stimul 6:409–415.

Hariri AR, Tessitore A, Mattay VS, Fera F, Weinberger DR (2002) The amygdala response to emotional stimuli: a comparison of faces and scenes. Neuroimage 17:317–323.

Henigsberg N, Kalember P, Petrović ZK, Šečić A (2019) Neuroimaging research in posttraumatic stress disorder - focus on amygdala, hippocampus and prefrontal cortex. Prog Neuropsychopharmacol Biol Psychiatry 90:37–42.

Hoang-Dang B, et al. (2024) Transcranial focused ultrasound targeting the amygdala may increase psychophysiological and subjective negative emotional reactivity in healthy older adults. Biol Psychiatry Glob Open Sci 4: 100342.

Hoffman KL, Gothard KM, Schmid MC, Logothetis NK (2007) Facial-expression and gaze-selective responses in the monkey amygdala. Curr Biol 17: 766–772.

Hur J, Stockbridge MD, Fox AS, Shackman AJ (2019) Dispositional negativity cognition, and anxiety disorders: an integrative translational neuroscience framework. Prog Brain Res 247:375–436.

Isbell LA (2006) Snakes as agents of evolutionary change in primate brains. J Hum Evol 51:1–35.

Isbell LA (2009) *The fruit, the tree, and the serpent: why we see so well*. Cambridge, MA: Harvard University Press.

Izquierdo A, Suda RK, Murray EA (2005) Comparison of the effects of bilateral orbital prefrontal cortex lesions and amygdala lesions on emotional responses in rhesus monkeys. J Neurosci 25:8534–8542.

Izquierdo A, Darling C, Manos N, Pozos H, Kim C, Ostrander S, Cazares V, Stepp H, Rudebeck PH (2013) Basolateral amygdala lesions facilitate reward choices after negative feedback in rats. J Neurosci 33:4105–4109.

Kalin NH, Shelton SE, Davidson RJ, Kelley AE (2001) The primate amygdala mediates acute fear but not the behavioral and physiological components of anxious temperament. J Neurosci 21:2067–2074.

Kamali A, Milosavljevic S, Gandhi A, Lano KR, Shobeiri P, Sherbaf FG, Sair HI, Riascos RF, Hasan KM (2023) The cortico-limbo-thalamo-cortical circuits: an update to the original Papez circuit of the human limbic system. Brain Topogr 36:371–389.

Koek RJ, et al. (2024) Deep brain stimulation of the amygdala for treatment-resistant combat post-traumatic stress disorder: long-term results. J Psychiatr Res 175:131–139.

Kolla NJ, Patel R, Meyer JH, Chakravarty MM (2017) Association of monoamine oxidase-a genetic variants and amygdala morphology in violent offenders with antisocial personality disorder and high psychopathic traits. Sci Rep 7:9607.

Konoike N, Iwaoki H, Nakamura K (2020) Potent and quick responses to conspecific faces and snakes in the anterior cingulate cortex of monkeys. Front Behav Neurosci 14:156.

Kubanek J, Shukla P, Das A, Baccus SA, Goodman MB (2018) Ultrasound elicits behavioral responses through mechanical effects on neurons and ion channels in a simple nervous system. J Neurosci 38:3081–3091.

Kubanek J, Brown J, Ye P, Pauly KB, Moore T, Newsome W (2020) Remote, brain region-specific control of choice behavior with ultrasonic waves. Sci Adv 6:eaaz4193.

Langevin JP, Chen JWY, Koek RJ, Sultzer DL, Mandelkern MA, Schwartz HN, Krahl SE (2016) Deep brain stimulation of the basolateral amygdala: targeting technique and electrodiagnostic findings. Brain Sci 6:28.

Lebow MA, Chen A (2016) Overshadowed by the amygdala: the bed nucleus of the stria terminalis emerges as key to psychiatric disorders. Mol Psychiatry 21:450–463.

Lee W, Lee SD, Park MY, Yang J, Yoo SS (2014) Evaluation of polyvinyl alcohol cryogel as an acoustic coupling medium for low-intensity transcranial focused ultrasound. Int J Imaging Syst Technol 24:332–338.

Legon W, Sato TF, Opitz A, Mueller J, Barbour A, Williams A, Tyler WJ (2014) Transcranial focused ultrasound modulates the activity of primary somatosensory cortex in humans. Nat Neurosci 17:322–329.

Legon W, Ai L, Bansal P, Mueller JK (2018) Neuromodulation with single-element transcranial focused ultrasound in human thalamus. Hum Brain Mapp 39:1995–2006.

Mahdavi KD, et al. (2023) A pilot study of low-intensity focused ultrasound for treatment-resistant generalized anxiety disorder. J Psychiatr Res 168: 125–132.

Matt E, Radjenovic S, Mitterwallner M, Beisteiner R (2024) Current state of clinical ultrasound neuromodulation. Front Neurosci 18:1420255.

Murphy JE, Yanes JA, Kirby LAJ, Reid MA, Robinson JL (2020) Left, right, or bilateral amygdala activation? How effects of smoothing and motion correction on ultra-high field, high-resolution functional magnetic resonance imaging (fMRI) data alter inferences. Neurosci Res 150:51–59.

Pennes HH (1948) Analysis of tissue and arterial blood temperatures in the resting human forearm. J Appl Physiol 1:93–122.

Plaksin M, Kimmel E, Shoham S (2016) Cell-type-selective effects of intramembrane cavitation as a unifying theoretical framework for ultrasonic neuromodulation. eNeuro 3:ENEURO.0136-15.2016.

Rabellino D, Densmore M, Harricharan S, Jean T, McKinnon MC, Lanius RA (2018) Resting-state functional connectivity of the bed nucleus of the stria terminalis in post-traumatic stress disorder and its dissociative subtype. Hum Brain Mapp 39:1367–1379.

Rascu M, Algermissen J, Weber L, Boer Td, Rushworth M, Klein-Flügge M (2025) Deep transcranial ultrasonic brain stimulation during decision-making in changing social-emotional environments. Brain Stimul 18: 410–411.

Rhodes SEV, Murray EA (2013) Differential effects of amygdala, orbital prefrontal cortex, and prelimbic cortex lesions on goal-directed behavior in rhesus macaques. J Neurosci 33:3380–3389.

Riis TS, Webb TD, Kubanek J (2022) Acoustic properties across the human skull. Ultrasonics 119:106591.

Riis TS, Feldman DA, Vonesh LC, Brown JR, Solzbacher D, Kubanek J, Mickey BJ (2023) Durable effects of deep brain ultrasonic neuromodulation on major depression: a case report. J Med Case Rep 17:449.

Riis TS, Losser AJ, Kassavetis P, Moretti P, Kubanek J (2024a) Noninvasive modulation of essential tremor with focused ultrasonic waves. J Neural Eng 21:016033.

Riis TS, Feldman DA, Losser AJ, Okifuji A, Kubanek J (2024b) Noninvasive targeted modulation of pain circuits with focused ultrasonic waves. Pain 165:2829–2839.

Robinson JL, Laird AR, Glahn DC, Lovallo WR, Fox PT (2010) Metaanalytic connectivity modeling: delineating the functional connectivity of the human amygdala. Hum Brain Mapp 31:173–184.

Rudebeck PH, Buckley MJ, Walton ME, Rushworth MFS (2006) A role for the macaque anterior cingulate gyrus in social valuation. Science 313:1310–1312.

Rutishauser U, Tudusciuc O, Neumann D, Mamelak AN, Heller AC, Ross IB, Philpott L, Sutherling WW, Adolphs R (2011) Single-unit responses selective for whole faces in the human amygdala. Curr Biol 21:1654–1660.

Saleem KS, Logothetis NK (2012) *A combined MRI and histology atlas of the rhesus monkey brain in stereotaxic coordinates*, Ed 2. San Diego, CA: Academic Press.

Sarica C, et al. (2022) Human studies of transcranial ultrasound neuromodulation: a systematic review of effectiveness and safety. Brain Stimul 15:737–746.

Steinhauer SR, Siegle GJ, Condray R, Pless M (2004) Sympathetic and parasympathetic innervation of pupillary dilation during sustained processing. Int J Psychophysiol 52:77–86.

Straube T, Mentzel HJ, Miltner WHR (2007) Waiting for spiders: brain activation during anticipatory anxiety in spider phobics. Neuroimage 37: 1427–1436.

Taubert J, Japee S (2024) Real face value: the processing of naturalistic facial expressions in the macaque inferior temporal cortex. J Cogn Neurosci 36: 2725–2741.

Webb TD, Wilson MG, Odéen H, Kubanek J (2022) Remus: system for remote deep brain interventions. iScience 25:105251.

Webb TD, Wilson MG, Odéen H, Kubanek J (2023) Sustained modulation of primate deep brain circuits with focused ultrasonic waves. Brain Stimul 16:798–805.